

Development and application of innovative triaxially braided ductile FRP fabric for strengthening concrete beams

Nabil F. Grace^{a,*}, Wael F. Ragheb^a, George Abdel-Sayed^b

^a Department of Civil Engineering, Lawrence Technological University, Southfield, MI 48075, USA

^b Department of Civil and Environmental Engineering, University of Windsor, Windsor, Ont., Canada N9B 3P4

Abstract

In this paper, an innovative triaxially braided ductile fiber reinforced polymer (FRP) fabric has been developed for strengthening reinforced concrete beams. The fabric was designed to potentially avoid most of the drawbacks experienced by currently available FRP strengthening systems. The ideal characteristics of a strengthening material for reinforced concrete beams were first investigated. Then, an analytical study was conducted to investigate the undulation effect of diagonal yarns on their loading behavior. Based on these investigations, the fabric was designed, manufactured, and its mechanical properties were experimentally evaluated. The effectiveness of the fabric as a strengthening material for reinforced concrete beams has been investigated by testing four reinforced concrete beams strengthened in flexure and shear using the new fabric. The test results showed that the fabric met its design objectives.

© 2003 Elsevier Ltd. All rights reserved.

Keywords: Concrete; Ductility; Strengthening; Braiding

1. Introduction

Several fiber reinforced polymer (FRP) systems are now commercially available for external strengthening of concrete structures. Fibers commonly used in these systems include glass, aramid, and carbon, and they are available in many forms such as pultruded plates, uniaxial fabrics, woven fabrics, and sheets. Although these materials have high strengths, they are very brittle. When loaded in tension, they exhibit a linear stress–strain relation up to failure without exhibiting a yield plateau or any indication of impending failure. The strain response of these materials is also different from that of conventional steel. Steel yields after elastically deforming to relatively low values of strain (0.2% for Grade 60 and 0.14% for Grade 40); while these FRP materials exhibit elastic deformation to relatively large strain values (compared to the yield strain of steel) before rupture. As a result, when they are used for flexural strengthening of concrete beams reinforced with conventional steel, some problems may be experienced. First, the steel reinforcement may yield before the

strengthening material provides any measurable contribution to the load of the beam. As a result, there is no improvement in beam yield load or stiffness. Second, when an increase in beam yield load or stiffness is required, larger cross sections of these materials must be used in order to contribute to the beam load when deformations are limited (before the steel yield). Moreover, brittle failures without significant yield plateaus are expected in these cases, due to debonding of the strengthening material from the surface of the concrete beam.

In beam shear strengthening applications, the FRP usually stretch to relatively low strain values (in comparison to their ultimate strains) before failure. Therefore, the benefits of the strengthening material are not fully realized. FRP materials are also highly orthotropic. They strengthen significantly only if loaded into the fiber direction. Therefore, for simultaneous flexure and shear strengthening of beams, more than one layer of these materials must be used.

Grace et al. [1] developed a uniaxial ductile FRP fabric that can be used to strengthen reinforced concrete beams in flexure. Although their fabric showed the potential to avoid most of the drawbacks experienced by the use of currently available FRP systems in strengthening reinforced concrete beams in flexure, it cannot be

* Corresponding author. Fax: +1-248-204-2568.

E-mail address: nabil@ltu.edu (N.F. Grace).

Nomenclature

b	beam width	V_f	composite fiber volume fraction
E_f	FRP elastic modulus	ε_{fe}	effective FRP strain
F_{fe}	effective FRP load per unit width	ρ_{frp}	FRP area fraction
s	axial yarn spacing	θ	braider angle
t_f	FRP thickness		

used for simultaneous flexural and shear strengthening of beams, as it contains fibers in only one direction. In this paper, the work of Grace et al. [1] has been extended to develop a triaxially braided ductile fabric. The fabric was developed to be used for strengthening reinforced concrete beams for flexure and/or shear. The fabric was designed to have the potential to offer the required flexural strengthening/stiffening level without significant ductility loss. In addition, it was designed to have the potential to be fully exploited when used for beam shear strengthening. The effectiveness of the fabric as a strengthening material for reinforced concrete beams has been verified by testing four reinforced concrete beams strengthened in flexure and shear using the developed fabric.

2. Ideal characteristics of a strengthening system

2.1. Flexural strengthening

Several experimental investigations [2–7] have been reported on the behavior of concrete beams strengthened in flexure using FRP sheets, plates or fabrics. In all these investigations, the strengthened beams showed higher ultimate loads in comparison to the non-strengthened ones. However, similar increases in beam yield loads were not noted. Because steel has a yield strain value less than the ultimate strain of the FRP, it yields before the FRP shows any significant contribution to beam load or stiffness. Accordingly, the strengthening material should exhibit its full strength at low strain values, preferably slightly more than the yield strain of the reinforcing steel, in order to contribute with its full strength simultaneously with the steel (being installed on the outer surface of the beam, the strengthening material undergoes slightly more strain than the inner reinforcing steel). On the other hand, the strengthening material should not rupture after reaching this strain value; otherwise a brittle failure will take place due to rupture of the FRP. Therefore, the strengthening material should have a high enough ultimate strain to guarantee that the beam will exhibit large deformations before failure, and hence enough ductility. In order to achieve these requirements, the strengthening material must

initially exhibit a linear stress–strain response up to a certain strain value. This strain value should be slightly greater than the yield strain of steel. Then, the strengthening material should exhibit an increase in strain without a corresponding increase in stress, similar to the yield phenomenon experienced by steel, up to a reasonable ultimate strain. Offering a yield plateau will indirectly help to avoid brittle beam failures that occur by either debonding of the FRP from the concrete surface or by shear–tension at the FRP end. Although these two modes of failures are rather complicated, the fact that FRP behaves in a linear elastic manner until failure is involved, in part, in causing such brittle failures. As the deformation of the beam increases, the tension in the FRP increases (because the FRP is linearly elastic and does not yield), requiring further anchorage. This is difficult to obtain, as the maximum anchorable FRP force is always limited. Therefore, by offering a yield plateau, the increase in the FRP tension force will be limited after yield and hence these two modes of failure will be avoided.

In view of these observations, the characteristics of an ideal FRP strengthening material for flexure can be summarized as follows:

1. It should initially exhibit a linear stress–strain response up to a certain strain value, then experience an increase in strain without a corresponding increase in stress, similar to the yield phenomenon experienced by steel.
2. The “yield strain” or “the yield-equivalent strain” should be slightly greater than the yield strain of steel.
3. The ultimate strain should be enough to guarantee enough beam deformation before FRP rupture.

2.2. Shear strengthening

Recent experimental investigations [8–13] showed that bonding FRP strips, fabrics, or sheets on the sides of beams improves their shear capacity. These investigations showed that when the strengthened concrete beam reaches its shear capacity, the FRP stretches to strain values that are usually small fractions of the FRP ultimate strain and hence the strength of the FRP is not fully exploited, which is not economical. Based on the

results of several reported experimental investigations, Triantafillou [13] expressed the maximum FRP strain before shear failure of the beam, the effective FRP strain (ϵ_{fe}), in terms of ($\rho_{frp}E_f$) as follows:

$$\epsilon_{fe} = 0.0119 - 0.0205(\rho_{frp}E_f) + 0.0104(\rho_{frp}E_f)^2$$

for $0 \leq \rho_{frp}E_f \leq 1$ GPa (1)

$$\epsilon_{fe} = 0.00245 - 0.00065(\rho_{frp}E_f) \quad \text{for } \rho_{frp}E_f > 1 \text{ GPa}$$

(2)

where ρ_{frp} is an FRP area fraction factor equal to $(2t/b)$, t is the FRP thickness, b is the beam width, and E_f is the FRP elastic modulus. By expressing E_f in terms of ϵ_{fe} and F_{fe} , where F_{fe} is the FRP load per unit width corresponding to the effective strain ϵ_{fe} , as $E_f = F_{fe}/(t \times \epsilon_{fe})$, the term $\rho_{frp}E_f$ can be rewritten as $2F_{fe}/(b \times \epsilon_{fe})$. Substituting in (1) and (2), the two equations can be rewritten as follows:

$$\epsilon_{fe} = 0.0119 - 0.0205\left(\frac{2F_{fe}}{b \cdot \epsilon_{fe}}\right) + 0.0104\left(\frac{2F_{fe}}{b \cdot \epsilon_{fe}}\right)^2$$

for $0 \leq \left(\frac{2F_{fe}}{b \cdot \epsilon_{fe}}\right) \leq 1$ GPa (3)

$$\epsilon_{fe} = 0.00245 - 0.00065\left(\frac{2F_{fe}}{b \cdot \epsilon_{fe}}\right)$$

for $\left(\frac{2F_{fe}}{b \cdot \epsilon_{fe}}\right) > 1$ GPa (4)

Based on Eqs. (3) and (4), the relationship between the effective strain (ϵ_{fe}) and the corresponding FRP load per unit width (F_{fe}) is calculated for different values of beam widths ($b = 0.125, 0.20, 0.30, 0.40$ m). This is shown in Fig. 1. Note from the figure that the contribution of the FRP to the beam's shear capacity can be optimized if it can provide a certain value of load at a strain of 0.5%.

In view of this, the shear strengthening material should exhibit its maximum strength at a strain value of 0.5%, with its corresponding load to be equal to the

optimum load discussed above. Since it is possible to install more than one layer of strengthening material on a beam, to get multiples of the load provided by one, it is better to have this load equal to the peak load of the smallest practical beam width (0.125 m for example).

Triantafillou [13] concluded that the effectiveness of the FRP increases as the fibers' direction becomes perpendicular to the diagonal crack. Accordingly, the strengthening system should have fibers at 45° to the longitudinal axis of the beam. The system would be ideal if it contained fibers at 0° for flexural strengthening and fibers in the $+45^\circ, -45^\circ$ directions for shear strengthening, all in the same layer. In this case, the orthotropic characteristics involved with using FRP materials would be no longer a problem for beam strengthening applications.

3. Development of a triaxially braided ductile fabric

A triaxially braided fabric has been developed. In this fabric, bundles of fibers were oriented in three different directions. These directions are $0^\circ, +45^\circ,$ and -45° . The 0° direction (referred to as the axial direction) acts mainly for flexural strengthening, while the $+45^\circ$ and -45° directions (referred to as the diagonal directions) act mainly for shear strengthening, in order to have fibers perpendicular to any potential shear cracks. A 2×2 triaxial braid pattern was used to combine the fiber bundles (yarns) in the three directions (Fig. 2). The 0° yarns are known as the "axial yarns", while the $\pm\theta$ yarns are known as the "braider yarns". The term "2x2" refers to the way diagonal yarns are intertwined; a $+\theta$ braider yarn continuously passes over two $-\theta$ braider yarns and then under two $-\theta$ braider yarns and vice versa, as shown in Fig. 2.

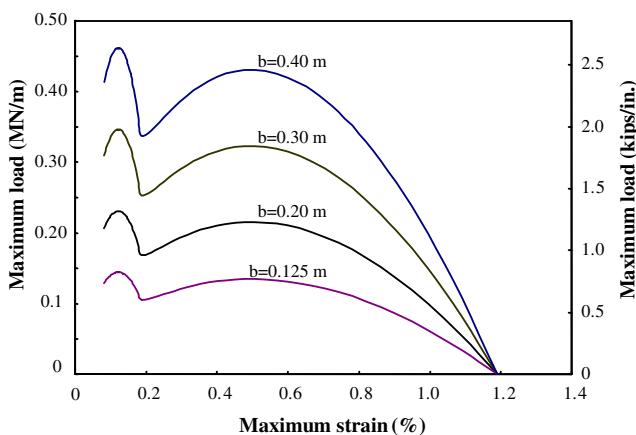


Fig. 1. Effective FRP strain and corresponding FRP load.

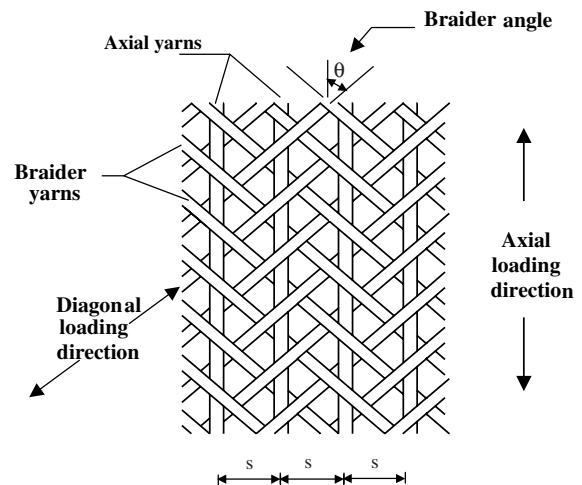


Fig. 2. 2x2 Triaxial braid pattern.

3.1. Method of analysis

NASA developed a general purpose analytical micromechanics technique to analyze textile composites [14,15]. This technique utilizes the periodicity of the textile composite to isolate a repeating unit cell (RUC) and then discretely models each yarn within the RUC. First, a three dimensional description of the textile composite is performed. The three dimensional effective stiffness of the composite is computed by discretizing each yarn in the RUC into yarn slices and using the material properties, spatial orientation, and volume fraction of each slice in a volume average technique that assumes an iso-strain state within the RUC. This analytical technique was implemented by Naik [16] in an analysis package called TEXCAD (TEXTile Composite Analysis for Design). TEXCAD has the ability to analyze different types of textile composites. TEXCAD was used to analyze and design the new fabric, with the permission of NASA.

3.2. Diagonal yarn undulation effect

In 2×2 triaxially braided fabrics (Fig. 2), the axial yarns are mainly straight, without any undulations; the diagonal yarns, however, are always undulating as they pass over and under the axial yarns. The undulation angle is known as the “crimp angle”. These undulations are expected to affect the diagonal loading behavior of these yarns. The main factors affecting the undulation geometry are the diagonal yarn size and the axial yarn spacing. An analytical study has been conducted to address the influence of these two factors on the diagonal loading behavior of the fabric. The study was conducted for three fiber types: (1) ultra high modulus carbon fibers (carbon #1), (2) high modulus carbon fibers (carbon #2), and (3) E-glass fibers. The composite mechanical properties of these fibers are listed in Table 1.

The effect of diagonal yarn size on the diagonal loading behavior of the composite fabric was studied. TEXCAD was used to analyze three models of triaxially braided fabrics with 45% fiber volume fraction, one for each type of fiber. In each case, the axial yarn size and spacing were kept constant as the diagonal yarn size

changed. The ultimate strain and ultimate load per unit width were calculated for the diagonal direction. The relation between diagonal yarn size and ultimate strain is plotted in Fig. 3. The relation between diagonal yarn

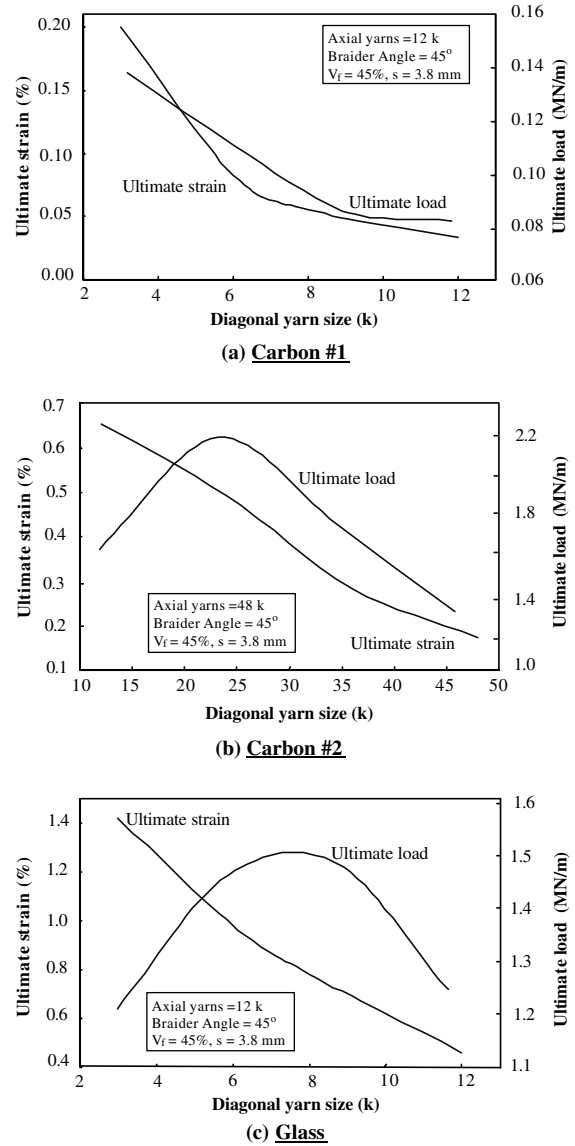


Fig. 3. Effect of diagonal yarn size on diagonal ultimate load and strain.

Table 1
Mechanical properties of the materials

Material	Description	Longitudinal modulus of elasticity, GPa (Msi)	Longitudinal tensile strength, MPa (ksi)	Failure strain, %	Transverse modulus of elasticity, GPa (Msi)	Filament diameter, μm
Carbon #1 ^a	Ultra-high modulus carbon fibers	379 (55)	1324 (192)	0.35	5.5 (0.8)	11
Carbon #2 ^a	High modulus carbon fibers	265 (38.5)	2200 (320)	0.8	10.3 (1.5)	5
Glass ^a	E-Glass fibers	48 (7)	1034 (150)	2.1	9.6 (1.4)	12.1
Epoxy	Resin	–	66.3 (9.6)	4.4	–	–

^a Composite properties based on 60% fiber volume fraction.

size and ultimate load is plotted in the same figure using a secondary axis. Note that the yarn sizes herein are measured in thousands of filaments (*k*). Clearly, as the diagonal yarn size increases the ultimate strain decreases. This is attributed to the increase in yarn crimp angle with the increase of yarn size. Note that carbon #1 is very sensitive to this effect (Fig. 3(a)). The ultimate strains are very low compared to the ultimate strain of this type of fiber. Therefore, diagonal yarn sizes should not be increased to the extent that the ultimate strain of the fabric becomes compromised. For the case of carbon #1, as diagonal yarn size increases, the ultimate load decreases. However, for carbon #2 and glass fibers, the ultimate load increases with the increase in diagonal yarn size due to the increase in its area. However after a certain size, it starts to decrease. This decrease in ultimate load is attributed to the increase in yarn crimp angle as the yarn size increases.

TEXCAD was used to study the effect of axial yarn size on the behavior of three diagonally loaded models, one for each fiber type. In each case, the axial and diagonal yarn sizes were kept constant and the axial yarn spacing was changed. The study was done for fabrics with 45% fiber volume fraction. The ultimate strain and ultimate load per unit width were calculated for each model. The effect of axial yarn spacing on ultimate strain is shown in Fig. 4. Clearly, ultimate strain increases with the increase of axial yarn spacing. This is attributed to the increase in undulation length as the axial yarn spacing increases. The relations between axial yarn spacing and ultimate load are plotted in Fig. 4 using a secondary axis. The figure indicates that ultimate load increases with increasing axial yarn spacing. However, after a certain point, the ultimate load starts to decrease with increasing axial yarn spacing (in the cases of carbon #2 and glass) or becomes constant (in the case of carbon #1). In cases of very small spacing, the diagonal strength of the fabric is almost lost.

3.3. Fabric design

In order to generate ductility, a hybridization technique was implemented in each direction. Three fibers were selected with different elongations to failure. By combining these fibers and controlling their mix ratio, the fibers with the lowest elongation (LE) fail first when loaded in tension, allowing a strain relaxation (that is, increase in strain without an increase in load). The remaining high elongation (HE) fibers then sustain the total load up to failure. The LE fiber strain at failure represents the value of the “yield-equivalent” strain of the hybrid, while the HE fiber strain at failure represents the ultimate strain. The load corresponding to failure of LE fibers represents the “yield-equivalent” load, and the maximum load carried by the HE fibers is the ultimate load. Medium elongation (ME) fibers were selected to

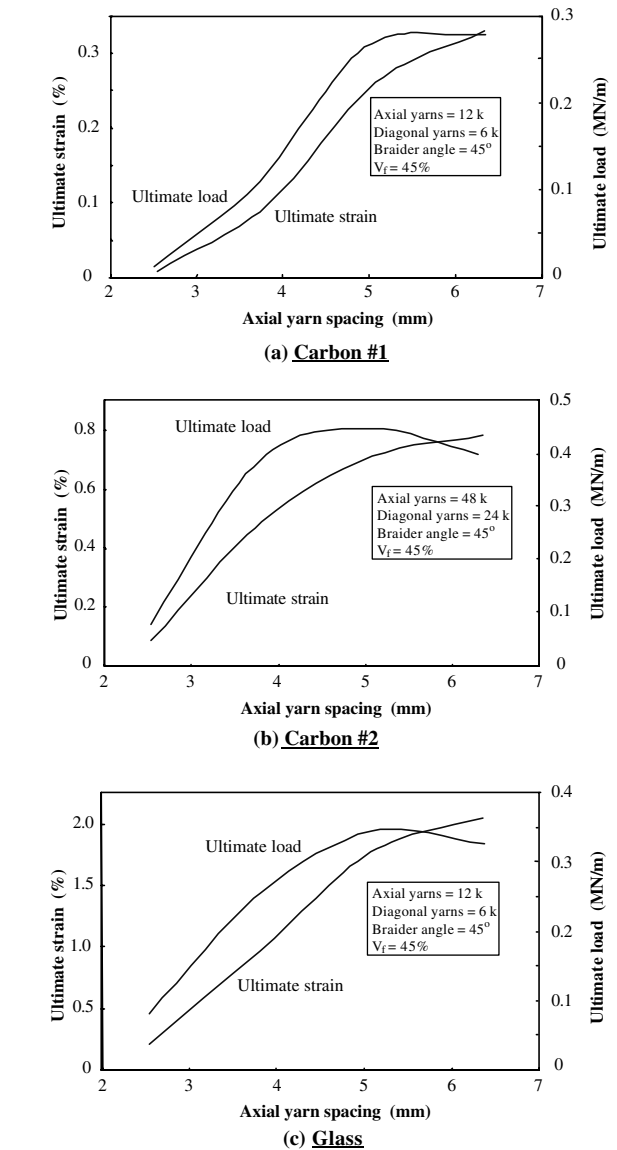


Fig. 4. Effect of axial yarn spacing on diagonal ultimate load and strain.

minimize the load drop that could occur after failure of the LE fibers during the strain relaxation, and also to provide a gradual load transition from the LE fibers to the HE fibers.

For the axial group of fibers (the 0° group), three different types of fibers were used. The first type was ultra high modulus carbon fiber (carbon #1), used as the LE fiber. The second type was high modulus carbon fiber (carbon #2), used as the ME fiber. The third type was E-glass fiber, used as the HE fiber. The fabric was designed so that when it is loaded in the axial direction (0°), it exhibits a linear load–strain behavior up to 0.35% strain, and then exhibits an increase in strain without a corresponding increase in load up to failure.

For the two diagonal groups (+45° and –45°), only two types of fibers were used. The first type was high

modulus carbon fiber (carbon #2), used as the ME fiber. The second type was E-glass fiber, used as the HE fiber. Herein, the ductility generation technique was similar to that of the axial direction, but with only one strain relaxation. The level of yarn undulation was controlled so that the undulated ME diagonal yarns failed first at a strain of 0.5%, with a corresponding load of 0.12 MN/m, which is the peak load of the smallest practical beam width as discussed earlier (Fig. 1). Failure of the ME yarns causes a strain relaxation. The level of undulation of the HE yarns was controlled to allow these yarns to sustain the total load up to failure at a strain value greater than 1.5%. The diagonal yarn sizes and axial yarn spacing were selected so that they did not exceed the limit discussed earlier in Figs. 3 and 4, where any increase in the yarn sizes or yarn spacing does not lead to a corresponding increase in the ultimate load capacity.

The design was done by first selecting a preliminary fabric geometry and then using *TEXCAD* to predict the tensile loading behavior of the fabric and comparing it with the design requirements. The geometry was then modified and *TEXCAD* was used to predict the loading behavior again. This procedure was repeated until the selected geometry fit the design requirements. The final geometry of the fabric is shown in Fig. 5. A photo of the fabric is shown in Fig. 6. The predicted load–strain behaviors of the fabric in both the axial and diagonal directions are plotted in Fig. 7.

3.4. Fabric testing

Epoxy impregnated samples of this fabric were tested according to ASTM D 3039 [17]. Two groups of samples were prepared. The first group was used to investigate the load–strain response of the fabric in the axial di-



Fig. 6. Photo of the triaxial fabric.

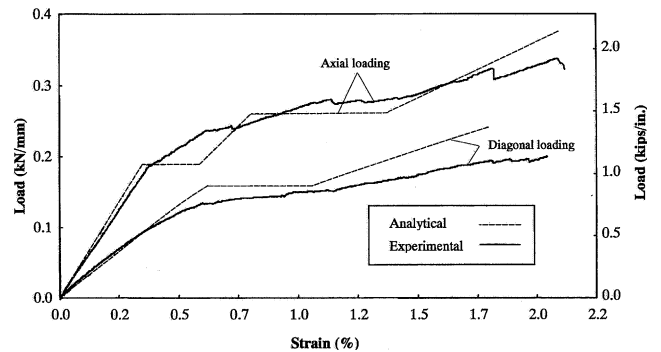


Fig. 7. Experimental and analytical tensile behavior of the triaxial fabric.

rection. In this group, samples were prepared so that the axial yarns were parallel to the direction of loading. The second group was used to investigate the load–strain response of the fabric in the diagonal directions. The samples were prepared so that one set of diagonal yarns

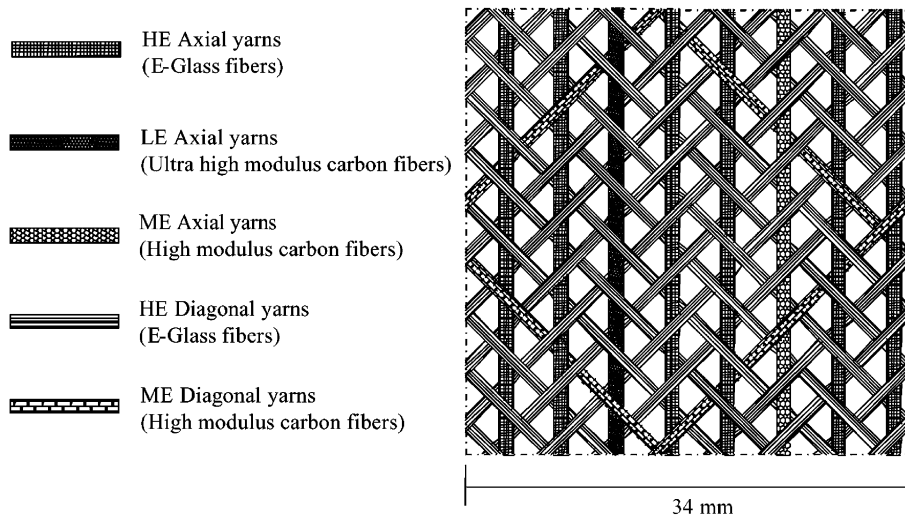


Fig. 5. Details of RUC geometry of the triaxial fabric.

was parallel to the direction of loading. Fig. 7 shows the experimental tensile load–strain response of the fabric in both the axial and diagonal directions, together with the theoretical predictions. The experimental results shown in the figure are the average results of three samples tested in each direction. Note that for axial loading, the fabric exhibited a linear load–strain behavior up to a strain of 0.38%, when the axial LE yarns failed. After this point, the strain started to increase in a faster rate than the load until failure occurred. For diagonal loading, the load–strain curve was almost linear up to a strain of 0.50%, when the diagonal LE yarns failed. At this point, an increase in strain occurred without a corresponding increase in load until total failure of the fabric occurred. The theoretical prediction was in a good agreement with the experimental results.

4. Experimental program

The experimental program contained two beam groups. The beams in group A were designed to investigate the fabric behavior in flexural strengthening, while the beams in group B were designed to investigate the fabric behavior in shear strengthening. The beams of Group A had cross sectional dimensions of 152 mm \times 3254 mm (6 in. \times 310 in.) and lengths of 2744 mm (108 in.), while group B beams had cross sectional dimensions of 152 mm \times 3280 mm (6 in. \times 311 in.) and lengths of 2744 mm (108 in.). All beams had a flexural reinforcement of two #5 (16 mm) tension bars near the bottom and two #3 (9.5 mm) compression bars near the top. The beams of group A were over-reinforced for shear with #3 (9.5 mm) closed stirrups spaced at 102 mm (4.0 in.), while the beams of group B were deficient in shear; they were reinforced with #3 (9.5 mm) closed stirrups spaced at 295 mm (11.63 in.). The beams were formed with rounded corners of 25 mm (1 in.) radius between the bottom face and the sides in order to allow wrapping the beam without stress concentrations. Fig. 8 shows the beam dimensions, reinforcement details, and loading set up. The compressive strength of the concrete at the time the beams were tested was 41.5 MPa (6000 psi).

The beams were prepared by sandblasting their surfaces to roughen them, cleaned with an air nozzle, and finally wiped to remove any dust or loose particles. The epoxy used to install the fabric has an ultimate tensile strength of 66.2 MPa (9.62 ksi) with an ultimate strain of 4.4% and a compressive strength of 109.2 MPa (15.84 ksi). The epoxy was allowed to cure for at least two weeks before the beams were tested. Table 2 summarizes details of the test beams.

Flexural strengthening beams, Group A and Group B, were instrumented with three strain gages on each beam located at the bottom face of the beam to measure the FRP strain at midspan. Shear strengthening beams,

Group B, were instrumented with rosette strain gages located at the expected locations of shear cracks to measure the FRP strain at the beam sides. The deflection was measured at the midspan using string potentiometers. The beams were loaded using a hydraulic actuator. The load was measured by means of a load cell. A data acquisition system was used to scan and record the readings from all the sensors.

5. Test results and discussion

5.1. Group A

The control beam (control A) had a yield load of 77 kN (17.3 kips) and an ultimate load of 87 kN (19.6 kips). The beam failed by yielding of steel followed by compression failure of concrete at the midspan. Test results for the beam are shown in Fig. 9. The beam exhibited a ductility index (the ratio between the deflection at failure to the deflection at yield) of 2.75.

Beam F-U75-1 was U-wrapped with one layer of the triaxial fabric along its bottom face, which was extended 152 mm (6 in.) up both sides. The fabric was installed for 1.83 m (72 in.), centered along the length of the beam. Test results for this beam are shown in Fig. 9. The beam yielded at a load of 112 kN (25.2 kips), an increase of 45% over the yield load of the control beam. The beam failed at a load of 133 kN (29.9 kips) due to compression failure of the concrete near the midspan with an increase of 53% over the failure load of the control beam. Unlike the behavior of currently available FRP systems, the triaxial fabric was able to offer a level of yield load increase that was very close to that of the ultimate load. As a result, beam F-U75-1 showed a yield plateau similar to that exhibited by the control beam. The ductility index of the beam was 2.33, which was 16% less than that of the control beam. It can be noted from the FRP strain diagram in Fig. 9(b) that the beam yielded at a fabric strain of 0.40%, which indicates that yielding of the fabric happened simultaneously with that of the steel reinforcement of the beam. The failed beam is shown in Fig. 10.

5.2. Group B

The control beam (control B) initially exhibited some tension cracks in the constant moment region near the midspan. Then, large diagonal cracks were formed in the constant shear span at a load of 88 kN (19.8 kips), which led to shear failure of the beam at a load of 100 kN (22.4 kips). Test results for this beam are shown in Fig. 11.

Beam FS-B3U was strengthened with three layers of triaxial fabric on the beam bottom face and one layer on each side. The fabric was installed for 2.26 m (89 in.)

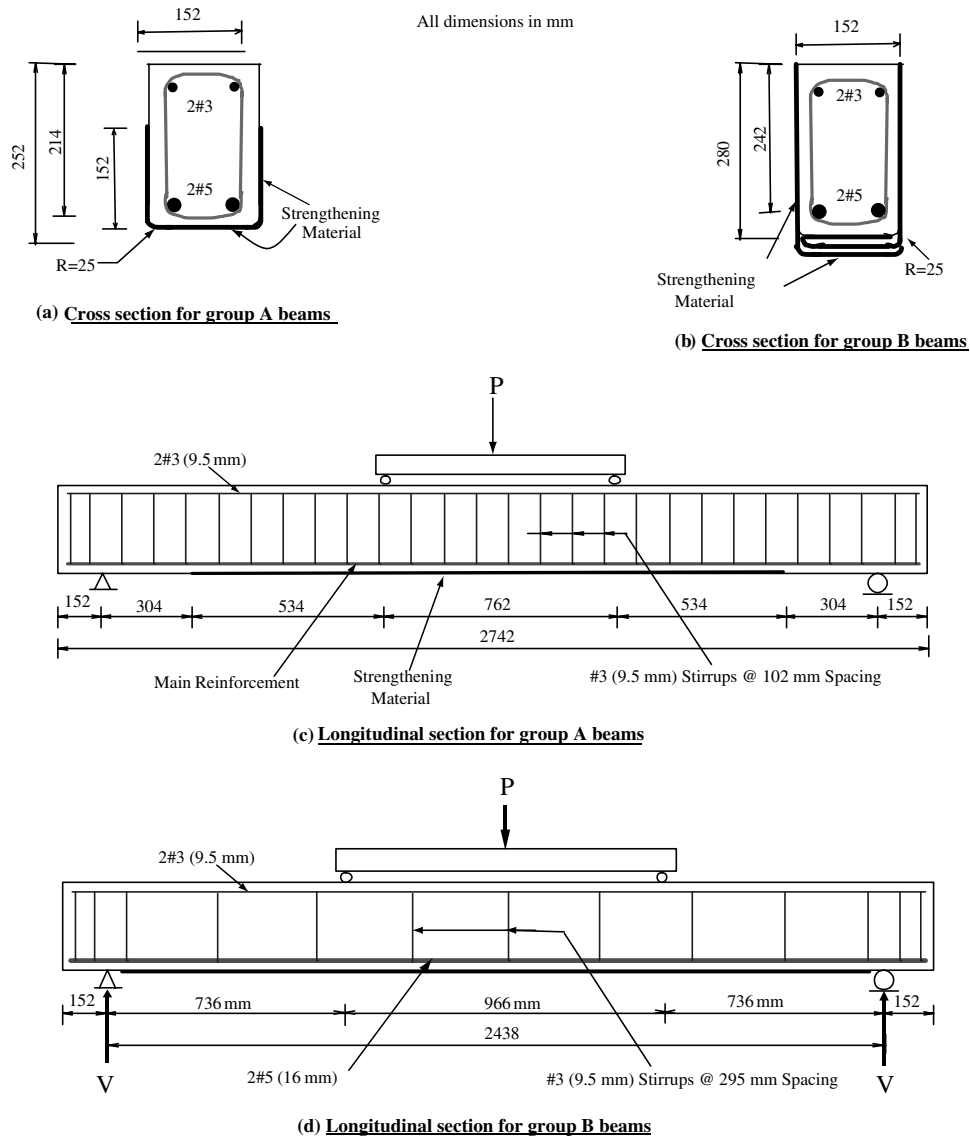


Fig. 8. Details of test beams of group A and group B.

Table 2
Summary of test beams

Beam group	Beam designation	Flexure or shear	Shear span	Strengthening scheme	Strengthening material
Group A	Control A	Flexure	838 mm (33 in.)	N/A	N/A
	F-U75-2			U-wrap	Triaxial fabric (1 layer)
Group B	Control B	Shear	736 mm (29 in.)	N/A	N/A
	FS-B3U			U-wrap	Triaxial fabric (1 layer at sides + 3 layers at bottom)

centered along the length of the beam. Test results for this beam are shown in Fig. 11. The beam failed by debonding of the fabric, followed by shear failure in the constant shear zone at a load of 180 kN (40.5 kips). The rosette strain gages showed a 45° strain value of 0.45%

before the beam failed, which was very close to the yield-equivalent strain value of the fabric in its diagonal direction. This indicates that failure of the beam happened almost simultaneously with the fabric yield, so the design objectives were met. The failed beam is shown in Fig. 12.

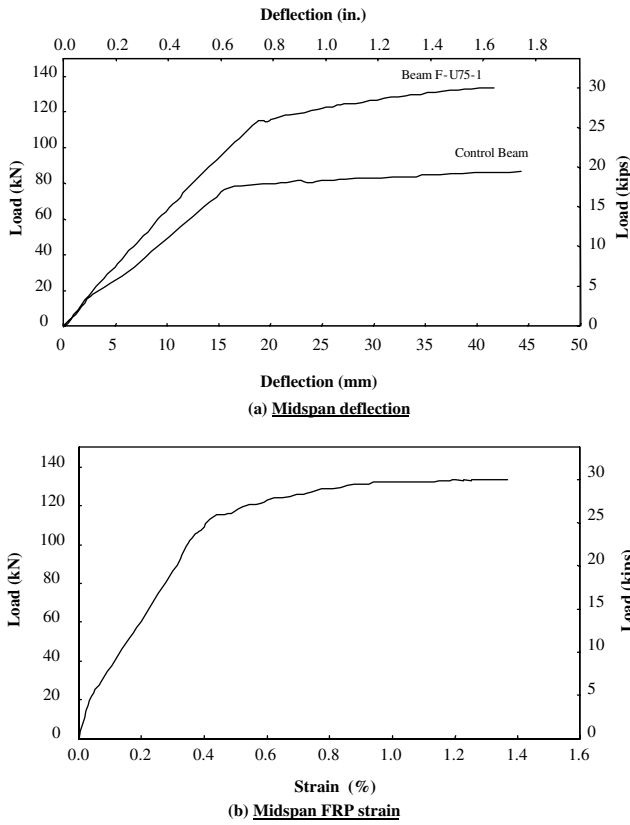


Fig. 9. Test results for beam F-U75-1.



Fig. 10. Failure of beam F-U75-1.

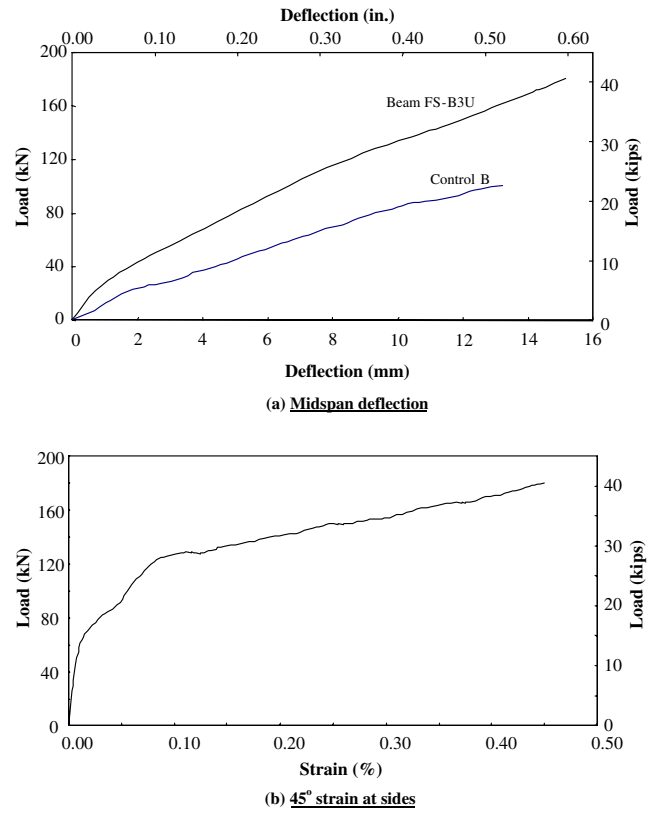


Fig. 11. Test results for beam FS-B3U.



Fig. 12. Failure of beam FS-B3U.

6. Conclusions

A triaxial ductile FRP strengthening system for concrete beams has been developed for applications that require shear and/or flexural strengthening. The system is a fabric that contains fibers braided in three different directions (0°, +45°, and -45°). It was designed to offer strength, stiffness, and ductility if loaded axially or diagonally. An analytical study was conducted on the behavior of triaxially braided fabrics. The study showed that the undulation of diagonal yarns may cause these yarns to fail at low strain values compared to the ultimate strain of the fiber. In addition, increasing the diagonal yarn sizes may not result in a corresponding increase in the beam's/fabric's load capacity because of the effect of yarn undulation. In view of this, a fabric geometry was selected and the load-strain diagrams of the fabric in the axial and diagonal direction were analytically predicted. The fabric was manufactured and tested in tension, and the load-strain diagrams were in a good agreement with the analytical prediction. The effectiveness of the fabric as a strengthening material for reinforced concrete beams has been investigated by

mate strain of the fiber. In addition, increasing the diagonal yarn sizes may not result in a corresponding increase in the beam's/fabric's load capacity because of the effect of yarn undulation. In view of this, a fabric geometry was selected and the load-strain diagrams of the fabric in the axial and diagonal direction were analytically predicted. The fabric was manufactured and tested in tension, and the load-strain diagrams were in a good agreement with the analytical prediction. The effectiveness of the fabric as a strengthening material for reinforced concrete beams has been investigated by

testing four reinforced concrete beams strengthened in flexure or shear. The test results showed that the beam strengthened in flexure did not exhibit a significant amount of ductility loss and the percentage of gain in beam yield load was very close to that of the ultimate load. The beam exhibited a yield plateau similar to that of the unstrengthened beam. The beam strengthened in flexure reached its shear capacity simultaneously with fabric yield, which indicated that the fabric met its design objectives.

Acknowledgements

This research has been conducted at the Structural Testing Center at Lawrence Technological University, Southfield, Michigan, USA, and was funded by the National Science Foundation under grant no. CMS-9906404 awarded to the first author. The assistance of Diversified Composites, Inc., Erlanger, Kentucky, is greatly appreciated. The authors wish to thank Shelby Precast Concrete, Shelby Township, Michigan for contributing the test beams. The features of the developed triaxially braided ductile fabric, as well as certain applications for the fabric, are the subject of a pending vs patent application.

References

- [1] Grace NF, Abdel-Sayed G, Ragheb WF. Strengthening of concrete beams using innovative ductile fiber-reinforced polymer fabric. *ACI Struct J* 2002;99(5):672–700.
- [2] Saadatmanesh H, Ehsani MR. RC beams strengthening with GFRP plates I: experimental study. *J Struct Eng* 1991;117(11):3417–33.
- [3] Ritchie PA, Thomas DA, Lu L, Connelly GM. External reinforcement of concrete beams using fiber reinforced plastics. *ACI Struct J* 1991;88(4):490–500.
- [4] Triantafillou TC. Strengthening of RC beams with epoxy-bonded-fiber-composite materials. *Mater Struct* 1992;25:201–11.
- [5] Norris T, Saadatmanesh H, Ehsani MR. Shear and flexure strengthening of R/C beams with carbon fiber sheets. *J Struct Eng* 1997;123(7):903–11.
- [6] Arduini M, Tommaso AD, Nanni A. Brittle failure in FRP plate and sheet bonded beams. *ACI Struct J* 1997;94(4):363–70.
- [7] Bencardino F, Spadea G, Swamy N. Strength and ductility of reinforced concrete beams externally reinforced with carbon fiber fabric. *ACI Struct J* 2002;99(2):163–71.
- [8] Chajes MJ, Januszka TF, Mertz DR, Thomson TA, Finch WW. Shear strengthening of reinforced concrete beams using externally applied composite fabric. *ACI Struct J* 1995;92(3):295–303.
- [9] Sato Y, Ueda T, Kakuta Y, Tanaka T. Shear reinforcing effect of carbon fiber sheet attached to side of reinforced concrete beams, in: El-Badry MM, editor. *Advanced Composite Materials in Bridges and Structures*. The Canadian Society of Civil Engineering; 1996. p. 621–7.
- [10] Araki N, Matsuzaki Y, Nakano K, Kataoka T, Fukuyama H. Shear capacity of retrofitted RC members with continuous fiber sheets, in: *Non-Metallic (FRP) Reinforcement for Concrete Structures*. Japan Concrete Institute; 1997. p. 515–22.
- [11] Taerwe L, Khalil H, Matthys S. Behavior of RC beams strengthened in shear by external CFRP sheets, in: *Non-Metallic (FRP) Reinforcement for Concrete Structures*. Japan Concrete Institute; 1997. p. 483–90.
- [12] Umezu K, Fujita M, Nakai H, Tamaki K. Shear behavior of RC beams with aramid fiber sheet, in: *Non-Metallic (FRP) Reinforcement for Concrete Structures*. Japan Concrete Institute; 1997. p. 491–8.
- [13] Triantafillou TC. Shear strengthening of reinforced concrete beams using epoxy-bonded FRP composites. *ACI Struct J* 1998;95(2):107–15.
- [14] Naik RA. Analysis of woven and braided fabric reinforced composites. Hampton, Virginia: National Aeronautics and Space Administration, NASA CR-194930, 1994.
- [15] Naik RA. Failure analysis of woven and braided fabric reinforced composites. Hampton, Virginia: National Aeronautics and Space Administration, NASA CR-194981, 1994.
- [16] Naik RA. *TEXCAD-Textile composite analysis for design*. Hampton, Virginia: National Aeronautics and Space Administration, NASA CR-4639, 1994.
- [17] ASTM D 3039. Standard test method for tensile properties of polymer matrix composite materials. In: *Annual Book of ASTM Standards*, 2000;15.03:106–18.